Optimal Short-term Operation of a Cascaded Hydro-Solar Hybrid System: a Case Study in Kenya

Dimitra Apostolopoulou, *Member*, *IEEE* and Malcolm McCulloch, *Senior Member*, *IEEE*

***Abstract*—In this paper we propose an optimal dispatch scheme for a cascaded hybrid hydro-solar power system, i.e., a hydroelectric system coupled with solar generation, that maximises the head levels of each dam, and minimises the spillage effects. As a result more water is stored in the dams to meet a given amount of energy providing more flexibility to the system in dry months. This dispatch scheme is based on the development of a simplified hydroelectric power system model which has low computational burden and may be implemented for the short-term operation of a cascaded hydro-solar hybrid power system. To this end, the non-convex relationships that describe the system physical constraints, e.g., hydroelectric power output, are transformed into affine relationships; thus reducing the computational complexity. The transformations are based on the construction of convex envelopes around bilinear functions, piecewise affine functions, and exploitation of optimisation properties. We validate the proposed framework and quantify the benefits of coupling hydroelectric and solar resources in terms of live water volume in dams and amount of solar a system may withstand with the Tana river cascade located in Kenya through an analysis of incorporating actual system data.**

***Index Terms*—Cascaded Hydro-Solar Hybrid, Hydroelectric Power System Model, Convex Relaxation, Optimal Dispatch.**

I. Introduction

Over the last five years there has been a marked increase of renewable-based resource integration into the electric grid that leads to the gradual de-carbonization of the energy supply sector [1]. Solar generation is one of the most promising renewable-based resources due to its low cost as a result of the numerous solar installations driven by policy and market forces. There are various examples in the world that show that solar generation is competitive when compared with other types of generation, such as geothermal power resources. For instance, in Atacama desert, located in northern Chile, a 120MW solar plant sells energy at only 2.91 cents/kWh [2]. The reduction of the greenhouse emissions is an international aim (e.g., the recent Paris Agreement is dealing with greenhouse emissions mitigation) and the integration of renewable resources into the system serves this purpose.

However, renewable resources have unique characteristics and their integration raises several challenges into power systems operation due to their intermittency and variability. The variability of the renewable-based generation requires that the system has enough ramping capability to follow the net load variations in different time frames, ranging from seconds to hours. Furthermore, there is an increase in the need for balancing services as well as reserves for frequency control (e.g., [3], [4]). There are several technologies available that may satisfy these needs. Unfortunately, most of them are associated with either additional cost or partial loss of the energy output. In this regard, appropriate use of existing resources, such as hydroelectric power systems, without any extra cost are worth to be investigated. Hydroelectric power systems are fitting candidates since they have good ramping capability and energy storage possibility in form of hydro reservoirs. For instance, in Switzerland, hydroelectric power systems have been used to meet the seasonal effects of demand [5]. Thus, they may be used to smooth the output of renewable-based generation and resolve any potential problems caused to the grid due to their output variability and intermittency. In addition, solar generation (a special case of renewable-based generation) and hydroelectric power are negatively correlated and may complement each other to meet the demand; thus paving the way for the investigation of hybrid hydro-solar systems (e.g., [6, p. 144], [7]). A hybrid hydro-solar system may be defined as a hydroelectric system and solar generation that are co-located and operated as one dispatchable unit. Usually, these two systems are connected to the same substation; thus a newly built solar system takes advantage of the existing transmission capability built for the hydroelectric system (e.g., [8]). Other studies performed in Brazil also demonstrate the high complementarity of hydroelectric and solar resources [9], [10].

In this regard, hydroelectric power systems may be used as large "storage" devices for renewable generation. Several papers have addressed the problem of investigating the new role of hydroelectric power systems in the power systems paradigm. In [11] the coordination of hydroelectric systems and wind generators in order to minimise wind energy curtailments during congestion situations is analysed. A case study on using a cascaded hydropower system to firm wind generation is presented in [12]. In [7] the authors state that small hydropower stations are complementary with solar systems and propose alterations on the systems' design to increase their complementarity over time. A comparison between the performance of the hybrid hydro-solar system and a simple PV-system installation is presented in [13]. Furthermore, the authors in [14] show that hydroelectric systems play an important role in future power systems, where renewable resources are present, and support system adequacy in case of supply shortfall.

However, there are several challenges associated with the operation of hydroelectric power systems as "storage" devices for renewable resources both in the steady state as well as

D. Apostolopoulou is affiliated with the Department of Electrical and Electronic Engineering of City, University of London, London, UK EC1V 0HB; and M. McCulloch with the Department of Engineering Science of the University of Oxford, Oxford, UK OX1 3PJ. E-mail: dimitra.apostolopoulou@city.ac.uk, malcolm.mcculloch@eng.ox.ac.uk.

The work of the authors was supported in part by the Foreign & Commonwealth Office (FCO) under project PPF AFR 160011 and the Oxford Martin School programme of Integrating Large-scale Renewables for a Secure, Affordable and Sustainable Energy Future.

dynamic operation. For instance, their coordinated operation requires simplified models for hydroelectric power systems that can be solved fast. Hydroelectric power systems are usually coupled both electrically, i.e., they are used to meet the same load; and hydraulically, i.e., the water outflow from one hydroelectric power plant is a significant portion of the inflow to the downstream plants [15, Ch. 7]. Furthermore, independent system operators, who are responsible for the operation of hydroelectric power plants, do not usually have optimisation tools to efficiently use the generation resources, considering the nonlinearities inherent to the dispatch problem. In particular, the nonlinearities are due to the spatio-temporal coupling among reservoirs; and for every plant, the nonlinear dependence between the power output, the water discharged, and the head of the associated reservoir.

In [16] a global optimisation of the short term scheduling for hydroelectric power generation with mixed integer nonlinear programming formulation of a cascaded of hydro plants is presented. However, in a security constrained short-term hydrothermal dispatch problem for large-scale systems coupled with renewable resources simplified models are also necessary. These models provide a balance between accuracy and complexity; and may be used for the day-to-day operation of cascaded hydro-solar hybrid systems. In [17] the authors propose a multi-dimensional piecewise affine approximation of the hydroelectric power curve. The authors in [18] propose a semidefinite programming method to solve a hydrothermal coordination problem; they reformulate and relax the non-convex constraints associated with hydroelectric power system while guaranteeing global optimality. However there are certain shortcomings with the proposed dispatch models available in literature. More specifically, nonlinear optimisation problems (e.g., [19]) have challenges such as the ability to efficiently solve large-scale problems, convergence to global optimal solutions, and requiring initial solutions. Moreover, approaches that relax the nonlinear initial problem might still keep some complexity. For instance, in [17], the resulting formulation contains extra continuous and binary variables, and constraints that add cost in terms of computation and would likely be intractable for use in system operators [20]. Some work has been concentrated into convexifying the nonlinear problem and using semidefinite programming techniques (e.g., [18]) to solve it; however, semidefinite programming solutions have very bad scalability [21]. The simplification of a dispatch model for a hydroelectric power system is very useful for several applications. For instance, in order to model the uncertainty of water flows in the hydroelectric systems stochastic models need to be used which require extensive computational times to solve; thus, it is imperative to use as a starting basis a computationally efficient deterministic model. The need for faster computational times is stressed in [17] since the computational burden involved in a highly sophisticated modelling of hydroelectric power systems is very cumbersome

In this paper, we propose a short-term optimal dispatch framework for a cascaded hydro-solar hybrid power system. In particular, we utilise the hydroelectric power system to meet the net demand after taking into account the solar generation output and ramping considerations; and operate them as one dispatchable unit. The main objective is to use water efficiently, i.e., use the minimum amount of water to meet the energy target; thus increasing the water stored in the reservoirs. The proposed optimal dispatch scheme increases the volume of water in the dams which is beneficial in dry months and for irrigation purposes. The maximum efficiency of the hydroelectric power plant occurs when the reservoir is full because the power output for a given amount of water is higher. In this regard, we construct the hydroelectric system optimal dispatch by appropriately choosing the objective function, i.e., maximise the water level in the dam, and representing the physical and power balance constraints. The importance of the head levels in a hydroelectric system cascade is discussed in [22]. We should note that operating a reservoir near its maximum in terms of head levels might introduce less short-term flexibility of the hydroelectric power plant since if there are high inflows there will not be enough storage for the incoming water in the dams thus forcing the operators to spill water. In this regard, we include in the objective function the minimisation of the spillage effects (e.g., [23], [24]) and consider an extended time-horizon, e.g., a day, for the dispatch of hydroelectric power. Unfortunately, the constructed problem exhibits a linear objective function but non-convex (bilinear) constraints. This formulation needs to be relaxed in an efficient manner so that its actual implementation in the short-term operation of a cascaded hydro-solar hybrid power system is realistic. To this end, the non-convex terms are relaxed by the construction of convex envelopes around the bilinear functions; piecewise affine functions with diseconomies of scale; and exploitation of optimisation properties of the simplex method. We demonstrate the implementation of the proposed methodology in a real hydroelectric power system in Kenya, which consists of a cascade of five hydroelectric power plants. The deterministic optimal short-term operation of a cascaded hydro-solar hybrid system presented in this paper was used to develop a robust variant that takes into account uncertainty [25]. In particular, in [25] correlated probabilistic forecasts for the uncertain output of renewable resources were developed based on clustering and Markov chain techniques; and then incorporated in the robust variant of the optimal dispatch. The resulting optimisation problem was intractable due to the infinite number of constraints; using tools from robust optimisation, we reformulated the resulting problem in a tractable form that was amenable to existing numerical tools and showed that the computed dispatch was immunised against uncertainty.

The contributions of this paper may be outlined as follows: (i) developed a linear dispatch model for hydroelectric power systems; (ii) used the aforementioned model to operate a cascaded hybrid hydro-solar system as one dispatchable unit, and (iii) performed a detailed case study of the Tana river cascade in Kenya which consists of five hydroelectric power systems in order to validate the proposed approach. The advantages of (i) compared to other works is that it approximates the system behaviour in satisfactory levels, as shown in the results' section and is scalable to incorporate a large number of hydroelectric systems in a cascade. The high complementarity of hydro and solar systems has been identified as discussed in [9], [10]; however, the development of a framework to operate a cascaded hybrid hydro-solar system as one dispatchable unit has not been addressed in the literature. As for (iii) a carefully designed case study for the Tana river cascade is also missing from the literature.

The remainder of the paper is organised as follows; in

Section II, we present the preliminaries of hydroelectric power systems: power output determination, constraining factors, e.g., maximum live volume, maximum power output. Moreover, the cascading effect of a system of hydroelectric power systems and spillage constraints are explicitly modelled. In Section III, we formulate the optimal dispatch method by determining the objective function and the power balance constraints. In Section IV, we recast the original problem to a linear optimisation problem by relaxing the non-convex constraints. In Section V, we illustrate the proposed methodology through the Tana river cascade located in Kenya; and discuss why cascaded hydro-solar hybrid systems are beneficial. In Section VI, we make some concluding remarks and discuss on future work.

II. Hydroelectric System Model

In this section, we introduce the hydropower function and the scheduling constraints that are utilised to develop our framework. We consider a hydroelectric power system with N hydroelectric power plants indexed by $\mathscr{N} = \{1, \ldots, N\}$ that we wish to schedule for a time period $\mathscr{T} = \{1, \ldots, T\}$. We denote by Δt the time intervals between time $t+1$ and t, which cannot be smaller than half-hour, since only the steady-state system behaviour is modelled.

A. Hydroelectric Power Output

A hydroelectric power plant $i \in \mathscr{N}$ may be characterised by its input-output curves. The input is in terms of water discharge and the output is in terms of power generation. The power generated by a hydroelectric power plant depends on the characteristics of the net hydraulic head, i.e., the difference between the level of the reservoir and the tail water, and the water discharge. In particular, the power of a hydroelectric power plant i at time t is defined as

$$P_{H_i}(t) = \eta_i(t, h_i(t), q_i(t))\, \rho\, g\, h_i(t)\, q_i(t),\ \forall i \in \mathscr{N},\ \forall t \in \mathscr{T}, \tag{1}$$

where ρ is the density of the water in kg/m^3; g is the gravitational acceleration in m/s^2; $h_i(t)$ is the net head of water (the difference in water level between upstream and downstream of the turbine) of hydropower plant i at time t in m; $q_i(t)$ is the discharge of water of plant i during time t in m^3/s; $\eta_i(t, h_i(t), q_i(t))$ is the efficiency of the turbine generator at head $h_i(t)$ and discharge $q_i(t)$. We chose the subscript H in the notation to refer to hydroelectric power. In this formulation, we neglect the tailrace effects, i.e., the head-dependency of the hydroelectric power output is modelled as the difference between the forebay level and the average tailrace level. The water level at the reservoir is called the forebay level and the water level at the discharge is called the tailrace level (e.g., [16]).

The power output of each hydroelectric power plant $i \in \mathscr{N}$ is constrained by a minimum and a maximum output, i.e., $P^{\mathrm{m}}_{H_i} \leq P_{H_i}(t) \leq P^{\mathrm{M}}_{H_i}$, for all $t \in \mathscr{T}$. Similar statements are true for the head levels and the water discharge rates. Thus, we have that

$$P^{\mathrm{m}}_{H_i} \leq P_{H_i}(t) \leq P^{\mathrm{M}}_{H_i},\ \forall i \in \mathscr{N},\ \forall t \in \mathscr{T}, \tag{2}$$

$$h^{\mathrm{m}}_i \leq h_i(t) \leq h^{\mathrm{M}}_i,\ \forall i \in \mathscr{N},\ \forall t \in \mathscr{T}, \tag{3}$$

$$q^{\mathrm{m}}_i \leq q_i(t) \leq q^{\mathrm{M}}_i,\ \forall i \in \mathscr{N},\ \forall t \in \mathscr{T}. \tag{4}$$

The speed at which hydroelectric power systems may respond to the solar and load variability is based on their respective up-and-down ramping capabilities. We impose these requirements and introduce appropriate constraints. We assume that the unit has the same ramp up and down capability κ_i in MW/h. More specifically, the ramping constraints of a hydroelectric power plant i are given by

$$-\kappa_i \Delta t \leq P_{H_i}(t+1) - P_{H_i}(t) \leq \kappa_i \Delta t, \forall i \in \mathscr{N},\ \forall t \in \mathscr{T}. \tag{5}$$

B. Cascading Effect of Hydroelectric System

Another physical constraint that needs to be taken into consideration in the operation of a cascaded hydroelectric power system is the water balance between reservoirs. This balance equation relates the live volumes of the reservoirs, total discharges, spillages, and inflows. Evaporation and percolation losses may be included into the expected inflows; thus there is no need to be considered separately. Furthermore, in most cases there is a delay in the flow of water between reservoirs that needs to be accounted for in the modelling. A mathematical formulation of the water balance of the hydroelectric power system with the use of the hydraulic continuity equations is given below:

$$\begin{aligned} V_1(t) &= V_1(t-1) + \Delta t(r_1(t) - q_1(t) - s_1(t)), && (6)\\ V_2(t) &= V_2(t-1) + \Delta t(r_2(t) + q_1(t-\tau_1) + s_1(t-\tau_1) \\ &\quad -q_2(t) - s_2(t)), && (7)\\ &\vdots \\ V_N(t) &= V_N(t-1) + \Delta t(r_{N-1}(t) + q_{N-1}(t-\tau_{N-1}) \\ &\quad +s_{N-1}(t-\tau_{N-1}) - q_N(t) - s_N(t)), && (8) \end{aligned}$$

where $V_i(t)$ is the live volume of hydroelectric power plant i at the end of time t in m^3; τ_i is the time delay between reservoir i and $i+1$, i.e., the time water needs to travel from one to the other; $r_i(t)$ is the inflow into hydroelectric power plant i during time to t; $s_i(t)$ is the spillage discharge of hydroelectric power plant i during time to t. The inflows into a plant are a function of several parameters, e.g., rainfall or evaporation. Forecasting $r_i(t)$ is a challenging task on which several researchers have focused on (e.g., [26]). Some additional physical constraints that may be taken into consideration are the initial (V_i(start)) and terminal (V_i(end) reservoir storage volumes, i.e.,

$$\begin{aligned} V_i(1) &= V_i(\text{start}),\ \forall i \in \mathscr{N}, && (9)\\ V_i(T) &= V_i(\text{end}),\ \forall i \in \mathscr{N}, && (10) \end{aligned}$$

where V_i(start) and V_i(end) are given.

There are constraints associated with the reservoir storage volume limits of each hydroelectric power plant $i \in \mathscr{N}$, which are defined as

$$V^{\mathrm{m}}_i \leq V_i(t) \leq V^{\mathrm{M}}_i,\ \forall i \in \mathscr{N},\ t \in \mathscr{T}. \tag{11}$$

The modelling of water stored in a reservoir and its mapping to a certain head level is important since it relates (1) with (6)-(8). This relationship in most reservoirs is determined from topographical surveys of the dam site and is highly nonlinear (e.g., [27], [28]). We denote this relationship by

$$h_i(t) = \phi_i(V_i(t)), \forall i \in \mathscr{N},\ t \in \mathscr{T}. \tag{12}$$

It should be noted that this mapping may be approximated by a linear function when referring to short-term operation of hydroelectric systems since for small head level differences we have small volume differences.

III. Cascaded Hydro-Solar Optimal Dispatch

In this section, we formulate the cascaded hydro-solar hybrid optimal dispatch. To this end, we introduce how the solar generation is taken into consideration into the power balance constraint; justify what is the objective of the optimal dispatch and define it; and determine the optimisation problem.

A. Power Balance Constraint

The output of a hydroelectric power system is used to meet the net load at every time instant $t \in \mathscr{T}$. In this regard, we have

$$\sum_{i \in \mathscr{N}} P_{H_i}(t) = \Delta P_L(t), \forall t \in \mathscr{T}, \tag{13}$$

where $\Delta P_L(t)$ is the net load at time t. We use the net load definition since we wish to include in our formulation the effects of renewable resources. More specifically, solar PV generation will be considered and the construction of cascaded hydro-solar hybrid systems will be studied. We define $\Delta P_L(t)$ as $\Delta P_L(t) = P_L(t) - P_{PV}(t)$, where $P_L(t)$ is the load at time t and $P_{PV}(t)$ is the PV output at time t. In a case where the net load is negative, i.e., $\Delta P_L(t) < 0$, the power balance constraint (13) is modified to be $\sum_{i \in \mathscr{N}} P_{H_i}(t) = \max\{\Delta P_L(t), 0\}, \forall t \in \mathscr{T}$. Cases of oversupply, i.e., $P_{PV}(t) > P_L(t) \Rightarrow \Delta P_L < 0$, may be dealt by common oversupply practises. For example, demand may be shifted at certain times or other generators may decrease their output. Last resort would be to manually "curtail" solar production by disconnecting some panels off from the grid. However, this would result in wasting clean, zero-carbon energy. In this regard, when selecting the size of the solar system that would be installed to coordinate with a hydroelectric system; such considerations need to be taken into account.

B. Objective Function Formulation

In order to formulate the hydroelectric system optimal dispatch, we first need to define a set of requirements that the system must satisfy: (i) maximise the energy per cubic meter of water in the system, i.e., system efficiency, and (ii) minimise the spillage effects.

The maximum energy per cubic meter of water or efficiency of the hydroelectric power plant occurs when the reservoir is full. The main reason behind this statement is that for a given water discharge the higher the head the higher the power output as it may be seen in (1). To this end, we wish to maximise the head of each reservoir at every time instant, i.e., $h_i(t)$, for all $i \in \mathscr{N}, t \in \mathscr{T}$. We have

$$\sum_{t \in \mathscr{T}} \sum_{i \in \mathscr{N}} h_i(t), \tag{14}$$

with the variables as defined in Section II. It should be noted that we could add some weighting factors, i.e., ξ_i in the objective function to represent the different efficiency levels in the plants of the cascade. In this regard, the objective would now be $\sum_{t \in \mathscr{T}} \sum_{i \in \mathscr{N}} \xi_i h_i(t)$. The solution to this modified problem would be similar. Due to the marginal differences in efficiency levels this is not studied in this paper [27], [29]. Another aspect that affects the choice of the objective function is how a unit of water contributes to the energy or peaking potential of the cascade; this issue will be studied in future work.

The spilling of water may be seen as the discharge of a water amount without any power generation. In this regard, water spilled is water that is not used by the hydroelectric power system. The minimisation of the spillage effects is accomplished by including in the objective function the term $\overline{M} \sum_{t \in \mathscr{T}} \sum_{i \in \mathscr{N}} s_i(t)$. We have:

$$\overline{M} \sum_{t \in \mathscr{T}} \sum_{i \in \mathscr{N}} s_i(t), \tag{15}$$

with $\overline{M}$ a large positive constant and the remaining variables as defined in Section II. It is important to notice that the spillage effects are positive if and only if the live volume has reached its maximum value:

$$s_i(t)(V_i(t) - V_i^{\mathrm{M}}) = 0, \forall i \in \mathscr{N}, t \in \mathscr{T}, \tag{16}$$

$$s_i(t) \geq 0, \forall i \in \mathscr{N}, t \in \mathscr{T}. \tag{17}$$

Since all terms in the inner product in (16) have the same sign, $s_i(t)$ is forced to be zero when $V_i(t) < V_i^{\mathrm{M}}$. When $V_i(t) = V_i^{\mathrm{M}}$ by (6)-(8), $s_i(t) > 0$ when the net inflow to the dam, i.e., difference between outflows, such as water discharge rates, and inflows, is positive since $V_i(t) = V_i(t-1)$.

C. Optimal Dispatch Formulation

In Sections II, III-A, and III-B, we have identified the objective function and the constraints that will be included in the optimal dispatch formulation. In this regard, we use (14) and (15) to construct the objective function. The decision variables of the optimal dispatch are the live volumes $V_i(t)$; the head levels $h_i(t)$; the power output $P_{H_i}(t)$; the spillage $s_i(t)$; and the water discharge rates $q_i(t)$, for all $i \in \mathscr{N}$, and $t \in \mathscr{T}$. The hydroelectric power output is given by (1); the cascading constraints and initial and final live volumes by (6)-(10); the relationship between the head level and live volume by (12); the power balance including solar generation by (13); and the spillage effect constraint by (16). The lower and upper bounds of decision variables are included through (2)-(4), (11), and (17) and the ramping constraints given by (5).

$$\begin{aligned}
\max_{\substack{h_i(t), P_{H_i}(t), \\ s_i(t), q_i(t), V_i(t)}} \quad & \sum_{t \in \mathscr{T}} \sum_{i \in \mathscr{N}} h_i(t) - \overline{M} \sum_{t \in \mathscr{T}} \sum_{i \in \mathscr{N}} s_i(t) \\
\text{subject to} \quad & \sum_{i \in \mathscr{N}} P_{H_i}(t) = \Delta P_L(t), \forall t \in \mathscr{T}, \\
& P_{H_i}(t) = \eta_i(t, h_i(t), q_i(t)) \rho g h_i(t) q_i(t), \\
& \qquad \forall i \in \mathscr{N}, t \in \mathscr{T}, \\
& V_1(t) = V_1(t-1) + (r_1(t) - q_1(t) \\
& \qquad - s_1(t)))\Delta t, \forall t \in \mathscr{T} \setminus \{1, T\}, \\
& V_i(t) = V_i(t-1) + (r_{i-1}(t) + q_{i-1}(t - \tau_{i-1}) \\
& \qquad + s_{i-1}(t - \tau_{i-1}) - q_i(t) - s_i(t)))\Delta t, \\
& \qquad \forall i \in \mathscr{N} \setminus \{1\}, t \in \mathscr{T} \setminus \{1\}, \\
& V_i(1) = V_i(\text{start}), \ \forall i \in \mathscr{N},
\end{aligned}$$

$$
\begin{aligned}
&V_i(T) = V_i(\text{end}),\ \forall i \in \mathscr{N},\\
&h_i(t) = \phi_i(V_i(t)), \forall i \in \mathscr{N},\ t \in \mathscr{T},\\
&-\kappa_i \Delta t \leq P_{H_i}(t+1) - P_{H_i}(t) \leq \kappa_i \Delta t,\\
&\forall i \in \mathscr{N}, t \in \mathscr{T} \setminus \{T\},\\
&s_i(t)(V_i(t) - V_i^{\mathrm{M}}) = 0, \forall i \in \mathscr{N}, t \in \mathscr{T},\\
&q_i^{\mathrm{m}} \leq q_i(t) \leq q_i^{\mathrm{M}},\ \forall i \in \mathscr{N}, t \in \mathscr{T},\\
&h_i^{\mathrm{m}} \leq h_i(t) \leq h_i^{\mathrm{M}},\ \forall i \in \mathscr{N}, t \in \mathscr{T},\\
&P_{H_i}^{\mathrm{m}} \leq P_{H_i}(t) \leq P_{H_i}^{\mathrm{M}},\ \forall i \in \mathscr{N}, t \in \mathscr{T},\\
&s_i(t) \geq 0,\ \forall i \in \mathscr{N}, t \in \mathscr{T},\\
&V_i^{\mathrm{m}} \leq V_i(t) \leq V_i^{\mathrm{M}}, \forall i \in \mathscr{N},\ t \in \mathscr{T}. \qquad (18)
\end{aligned}
$$

The output of (18) determines the head levels, power output, volume, spillage and water discharge for every hydroelectric power plant at every time instant in the period of interest. As it may be seen (18) has a linear objective function with linear and nonlinear constraints. In (18) the number of decision variables is $5NT$; number of equality constraints is $4NT+T$; and number of inequality constraints is $2N(T-1)+9NT$. The challenge in (18) is that it is a non-convex optimisation problem since its equality constraints (e.g., the power output of the hydroelectric power plant) are non-convex functions. In order to solve (18) several algorithms may be used, e.g., gradient methods, however a global optimum is not guaranteed. Moreover, this optimisation problem provides the output of a cascaded hydro-solar hybrid power system in short-term operation; thus, highlights the necessity of efficient solution methodologies. To this end, we relax the original optimal dispatch problem given in (18).

IV. Relaxations of Optimal Dispatch

In this section, we describe how we relax each of the non-convex constraints into a convex form and in particular into affine constraints; as a result the optimal dispatch is transformed into a linear optimisation problem amenable to very efficient numerical tools. The non-convex constraints of (18) refer to (i) the output of a hydroelectric power system, i.e., $P_{H_i}(t) = \eta_i(t, h_i(t), q_i(t))\, \rho\, g\, h_i(t)\, q_i(t), \forall i \in \mathscr{N},\ t \in \mathscr{T}$; (ii) the spillage effects, i.e., $s_i(t)(V_i(t) - V_i^{\mathrm{M}}) = 0, \forall i \in \mathscr{N}, t \in \mathscr{T}$; and (iii) the mapping of the head level to the volume, i.e., $h_i(t) = \phi_i(V_i(t)), \forall i \in \mathscr{N},\ t \in \mathscr{T}$. In particular, we construct a convex envelope around the bilinear relationship of the hydroelectric power output; recast the spillage effects' constraint; and use a piecewise affine relationship connecting the head levels and the live volume of each dam.

A. Convex Envelope of Hydroelectric Output

The non-convex relationship of the output of a hydroelectric power system, the head and the water discharge is a bilinear function for a constant turbine efficiency. We assume the efficiency is constant, i.e., $\eta_i(t, h_i(t), q_i(t)) = \eta_i$ and replace the remaining bilinear terms with a convex envelope consisting of affine over- and underestimating inequality constraints to transform the non-convex constraint into a set of affine inequality constraints. This assumption is rational as demonstrated in the case study results section with the use of actual hydroelectric power plant data. In particular, we have that $P_{H_i(t)} = a_i\, h_i(t)\, q_i(t)$, with $a_i = \eta_i\, \rho\, g$, and $q_i^{\mathrm{m}} \leq q_i(t) \leq q_i^{\mathrm{M}}$, $h_i^{\mathrm{m}} \leq h_i(t) \leq h_i^{\mathrm{M}}$. By using McCormick's envelopes (e.g., [30]), we obtain:

$$
\begin{aligned}
P_{H_i}(t) &\geq a_i(q_i^{\mathrm{m}} h_i(t) + h_i^{\mathrm{m}} q_i(t) - h_i^{\mathrm{m}} q_i^{\mathrm{m}}), && (19)\\
P_{H_i}(t) &\geq a_i(q_i^{\mathrm{M}} h_i(t) + h_i^{\mathrm{M}} q_i(t) - h_i^{\mathrm{M}} q_i^{\mathrm{M}}), && (20)\\
P_{H_i}(t) &\leq a_i(q_i^{\mathrm{m}} h_i(t) + h_i^{\mathrm{M}} q_i(t) - h_i^{\mathrm{M}} q_i^{\mathrm{m}}), && (21)\\
P_{H_i}(t) &\leq a_i(q_i^{\mathrm{M}} h_i(t) + h_i^{\mathrm{m}} q_i(t) - h_i^{\mathrm{m}} q_i^{\mathrm{M}}). && (22)
\end{aligned}
$$

B. Spillage Effect Reformulation

The spillage effects, $s_i(t)$ are introduced with (6)-(8). We demonstrate how the constraints associated with spillage effects given in (16) may be dropped from (18). In the absence of spillage (6)-(8) would be satisfied with $s_i(t) = 0$. Thus, we may see $s_i(t)$ as an "artificial" variable that increases the feasible space of the problem and also has a physical meaning. The optimal dispatch objective function is designed to minimise the spillage effects, i.e., make $s_i(t) = 0$ when it is feasible. The same concept is true for the "artificial" variables in linear programming where penalty terms, e.g., with the use of the Big-M method (e.g., [31]), are added to the objective function to push out the "artificial" variables from the basic variables, i.e., basis. With the Big-M method in a minimisation problem, if $\overline{M}$ is large, then any basis that includes a positive artificial variable will lead to a large positive value of the objective function. If there is any basic feasible solution to the constraints of the original linear program, then the corresponding basis will not include any artificial variables and its objective value will be much smaller. Because the artificial variables have a high cost associated with them, the simplex method removes them from the basis if this is at all possible. Any basic feasible solution to the penalised problem in which all the artificial variables are nonbasic (and hence zero) is also a basic feasible solution to the original problem. The corresponding basis can be used as an initial basis for the original problem. Thus, we argue that by including $s_i(t)$ in the objective function multiplied with a large positive number $\overline{M}$, then it will non zero only when $V_i(t-1) + (r_{i-1}(t) + q_{i-1}(t - \tau_{i-1}))\Delta t > V_i^{\mathrm{M}} \Rightarrow V_i(t) > V_i^{\mathrm{M}}$. When $V_i(t) < V_i^{\mathrm{M}}$, then $s_i(t) = 0$ as explained above. As a result, the nonlinear constraint $s_i(t)(V_i(t) - V_i^{\mathrm{M}}) = 0$, $\forall i \in \mathscr{N}, t \in \mathscr{T}$ is satisfied and does not need to be included in (18).

C. Piecewise Affine Approximation of $h_i(t) = \phi_i(V_i(t))$

One of the most useful applications of the piecewise affine representation is for approximating nonlinear functions. In this regard, we convert the nonlinear mapping of the head level to the volume, i.e., $h_i(t) = \phi_i(V_i(t))$ to a piecewise affine relationship. We consider $k = 1, \ldots, K$ intervals and thus have:

$$
h_i(t) = \beta_i^k v_i^k(t) + \gamma_i^k, v_i^k(t) \in [\zeta_k, \zeta_{k+1}],\ \text{for } k = 1, \ldots, K, \qquad (23)
$$

where $\beta_i^k, \gamma_i^k \in \mathbb{R}^+ = \{x \in \mathbb{R} | x \geq 0\}$, for $k = 1, \ldots, K$, $\zeta_1 < \zeta_2 \cdots < \zeta_{K+1}$, $v_i^k(t) \in \mathbb{R}^+$ with $V_i(t) = \sum_{k=1}^{K} v_i^k(t)$. An analysis of the continuous piecewise affine approximation of the head to the volume of existing reservoirs based on data found in [32] showed that $\beta_i^1 > \beta_i^2 > \cdots > \beta_i^K$. Usually, piecewise affine functions are formulated as mixed integer programming problems, which would increase the complexity

of (18). However, a special case for representing piecewise affine functions arises when diseconomies of scale apply, i.e., when $\beta_i^1 > \beta_i^2 > \cdots > \beta_i^K$ and we are maximising $h_i(t)$, which is this case (e.g., [33]). Thus, (23) may be rewritten as

$$h_i(t) = \sum_{k=1}^{K}(\beta_i^k v_i^k(t)) + \gamma_i^1, v_i^k(t) \in [0, \zeta_{k+1} - \zeta_k], \text{ for } k = 1, \ldots, K. \quad (24)$$

Notice the slight abuse of notation with the term $v_i^k(t)$, which represents different quantities in (23) and (24); the interpretation will always be clear from the context.

D. Overall Framework

The proposed optimal dispatch of a hydroelectric power system given in (18) may be rewritten in its relaxed form as

$$\begin{aligned}
\max_{\substack{h_i(t), P_{H_i}(t),\\ s_i(t), q_i(t), v_i^k(t)}} \quad & \sum_{t\in\mathscr{T}}\sum_{i\in\mathscr{N}} h_i(t) - \overline{M}\sum_{t\in\mathscr{T}}\sum_{i\in\mathscr{N}} s_i(t) \\
\text{subject to} \quad & \\
& \sum_{i\in\mathscr{N}} P_{H_i}(t) = \Delta P_L(t), \forall t \in \mathscr{T}, \\
& P_{H_i}(t) \geq a_i(q_i^{\mathrm{m}} h_i(t) + h_i^{\mathrm{m}} q_i(t) - h_i^{\mathrm{m}} q_i^{\mathrm{m}}), \\
& \qquad \forall i \in \mathscr{N}, t \in \mathscr{T}, \\
& P_{H_i}(t) \geq a_i(q_i^{\mathrm{M}} h_i(t) + h_i^{\mathrm{M}} q_i(t) - h_i^{\mathrm{M}} q_i^{\mathrm{M}}), \\
& \qquad \forall i \in \mathscr{N}, t \in \mathscr{T}, \\
& P_{H_i}(t) \leq a_i(q_i^{\mathrm{m}} h_i(t) + h_i^{\mathrm{M}} q_i(t) - h_i^{\mathrm{M}} q_i^{\mathrm{m}}), \\
& \qquad \forall i \in \mathscr{N}, t \in \mathscr{T}, \\
& P_{H_i}(t) \leq a_i(q_i^{\mathrm{M}} h_i(t) + h_i^{\mathrm{m}} q_i(t) - h_i^{\mathrm{m}} q_i^{\mathrm{M}}), \\
& \qquad \forall i \in \mathscr{N}, t \in \mathscr{T}, \\
& \sum_{k=1}^{K} v_1^k(t) = \sum_{k=1}^{K} v_1^k(t-1) + (r_1(t) - q_1(t) \\
& \qquad - s_1(t))\Delta t, \forall t \in \mathscr{T} \setminus \{1\}, \\
& \sum_{k=1}^{K} v_i^k(t) = \sum_{k=1}^{K} v_i^k(t-1) + (r_{i-1}(t) \\
& \qquad + q_{i-1}(t - \tau_{i-1}) + s_{i-1}(t - \tau_{i-1}) \\
& \qquad - q_i(t) - s_i(t))\Delta t, \forall i \in \mathscr{N} \setminus \{1\}, \\
& \qquad t \in \mathscr{T} \setminus \{1\}, \\
& \sum_{k=1}^{K} v_i^k(1) = V_i(\text{start}), \ \forall i \in \mathscr{N}, \\
& \sum_{k=1}^{K} v_i^k(T) = V_i(\text{end}), \ \forall i \in \mathscr{N}, \\
& h_i(t) = \sum_{k=1}^{K}(\beta_i^k v_i^k(t)) + \gamma_i^1, \forall i \in \mathscr{N}, t \in \mathscr{T}, \\
& -\kappa_i \Delta t \leq P_{H_i}(t+1) - P_{H_i}(t) \leq \kappa_i \Delta t, \\
& \qquad \forall i \in \mathscr{N}, t \in \mathscr{T} \setminus \{T\}, \\
& q_i^{\mathrm{m}} \leq q_i(t) \leq q_i^{\mathrm{M}}, \ \forall i \in \mathscr{N}, t \in \mathscr{T}, \\
& P_{H_i}^{\mathrm{m}} \leq P_{H_i}(t) \leq P_{H_i}^{\mathrm{M}}, \ \forall i \in \mathscr{N}, t \in \mathscr{T} \\
& s_i(t) \geq 0, \ \forall i \in \mathscr{N}, t \in \mathscr{T}, \\
& 0 \leq v_i^k(t) \leq \zeta_{k+1} - \zeta_k, \forall i \in \mathscr{N}, \\
& \qquad t \in \mathscr{T}, k = 1, \ldots, K. \qquad (25)
\end{aligned}$$

It maybe be easily seen that (25) is a linear optimisation problem that may be solved with high computational efficiency. In (25) the number of decision variables is $4NT + KNT$; number of equality constraints is $2NT + T$; and number of inequality constraints is $2N(T-1) + 9NT + 2KNT$.

V. Case Study: Tana River Cascade

In this section, we illustrate the proposed optimal dispatch of a cascaded hydro-solar hybrid system with the cascaded hydroelectric plants of the Tana river in Kenya, which consists of five hydroelectric power plants from Masinga Main Reservoir to Kiambere [27], i.e., $\mathscr{N} = \{1, 2, \ldots, 5\}$. The time horizon we wish to schedule its operation is over one day, i.e., $\mathscr{T} = \{1, 2, \ldots, 24\}$, with hourly intervals, i.e., $\Delta t = 1$, for a one year period, i.e., we solve the daily scheduling optimisation problem 365 times, once for each day. The turbine generators efficiencies for the five dams are: $\eta_1(t) = \eta_1(t, h_1(t))$, $\eta_2(t) = 0.9$, $\eta_3(t) = 0.92$, $\eta_4(t) = 0.89$, and $\eta_5(t) = 0.9$, as depicted in Fig. 1. The constraints of the Tana river cascade in terms of power output, live volume, head, and ramping characteristics may be found in [32] and are shown in Table I. The minimum power output, live volume, and water discharge rate for all reservoirs are zero, i.e., $P_i^{\mathrm{m}} = 0$, $V_i^{\mathrm{m}} = 0$, $q_i^{\mathrm{m}} = 0$ for $i = 1, \ldots, 5$. The number of units each plant has is: Masinga 2; Kamburu 3; Gitaru 3; Kindaruma 3; and Kiambere 2. Determining the unit commitment of the units of each hydroelectric dam is out of the scope of the paper and the units' dispatch is assumed as given. For this case study the minimum power output of each dam was considered to be zero. However, since the turbines used in the Tana river cascade are Kaplan and Francis; a more realistic assumption would be to set the minimum power output to around 40% of nominal power output, which will be part of future work.

In the remaining section, we will present how accurate are the proposed relaxations and use the proposed optimal dispatch to meet the load for an entire year with the use of the hydroelectric power system. Next, we will add solar generation to the system, i.e., building a cascaded hydro-solar hybrid and quantify the associated benefits in terms of live dam water volume.

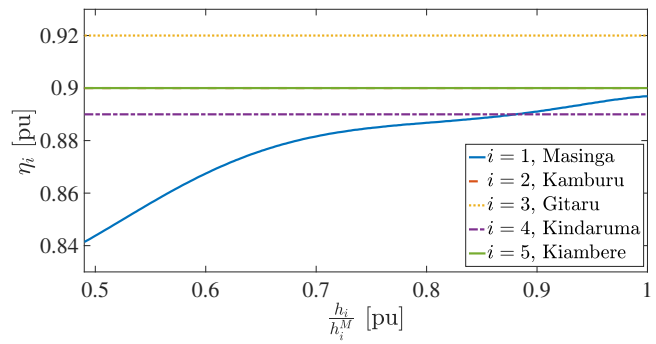

Fig. 1: Turbine efficiencies for the five dams.

TABLE I: Tana river cascade data.

Reservoir	Masinga	Kamburu	Gitaru	Kindaruma	Kiambere
P_i^{M} [MW]	40	93	225	72	165
V_i^{M} [Mm^3]	1753	133	21	10	519
h_i^{M} [m]	51	78	140	35	151
h_i^{m} [m]	25	61	131	31	134
q_i^{M} [m^3/s]	198.8	161.82	189	265.68	132
κ_i [MW/h]	36	64	182	64.62	142

TABLE II: Comparison of actual and approximated power output of each hydroelectric system, $\epsilon_i(t) = |P_{\text{actual}_i}(t) - P_{H_i}(t)|$.

Reservoir	Masinga	Kamburu	Gitaru	Kindaruma	Kiambere
$\mathbb{E}[\epsilon_i]$ [MW]	0.22	0.01	0.01	0.09	0.01
σ_i [MW]	0.63	0.06	0.04	0.25	0.11
$\frac{\mathbb{E}[\epsilon_i]}{P_i^{\mathrm{M}}}$ [%]	0.56	0.01	0.00	0.12	0.01

A. Accuracy of Relaxations

The national load duration curve of Kenya for 2011 is depicted in Fig. 2. In order to determine $P_L(t)$ for $t \in \mathscr{T}$ for the entire year, we need to make sure that the installed capacity of the hydroelectric power system is sufficient. Thus, we constrain the load to a maximum value of 500 MW $< \sum_{i=1}^{5} P_{H_i}^{\mathrm{M}}$. We will use the five hydroelectric power system to meet this load.

The relationship connecting the power output, the head and water discharge levels is given in (1). A graphic representation of this relationship for the Gitaru hydroelectric power station is given in Fig. 3. The motivation behind the choice of the objective function in Section III-B is clear through this graph, since for the same discharge level of water higher head levels produce more power. In Section IV-A, where the relaxation procedure is described there is the assumption that the turbine efficiencies are constant, i.e., $\eta_i(t, h_i(t), q_i(t)) = \eta_i$. The latter is a true statement for all the hydroelectric power plants besides Masinga, where the turbine efficiency is variable and is higher for higher head levels, as shown in Fig. 1. Thus, when solving the problem for each day we use the efficiency that corresponds to the initial head level, i.e., $\eta_1(t) = \eta_1(1, h_1(1))$ for all $t \in \mathscr{T}$.

Given that we have constant turbine efficiencies for all the hydroelectric power systems, we may construct the convex envelope of the hydroelectric output as described in Section IV-A. From Table I, we have that $q_3^{\mathrm{m}} = 0$ m^3/s, $q_3^{\mathrm{M}} = 189$ m^3/s, $h_3^{\mathrm{M}} = 140$ m, and $h_3^{\mathrm{m}} = 131$ m. We use (19)-(22), and we set $q_3 = 125$ m^3/s $= q_3(0)$ to

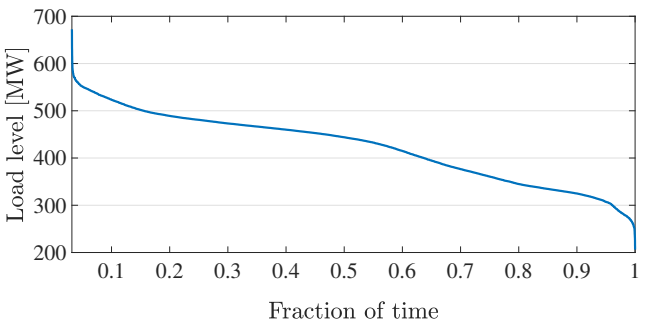

Fig. 2: National load duration curve of Kenya for 2011.

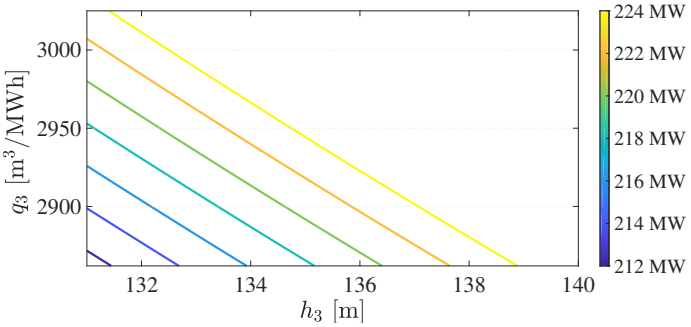

Fig. 3: Power output characteristic of Gitaru Dam in MW.

depict in Fig. 4 the convex envelope of the power output for the Gitaru hydroelectric power plant, for a given water discharge. In particular, $P_3^{(1)} = a_3(q_3^{\mathrm{m}} h_3 + h_3^{\mathrm{m}} q_3(0) - h_3^{\mathrm{m}} q_3^{\mathrm{m}})$; $P_3^{(2)} = a_3(q_3^{\mathrm{M}} h_3 + h_3^{\mathrm{M}} q_3(0) - h_3^{\mathrm{M}} q_3^{\mathrm{M}})$; $P_3^{(3)} = a_3(q_3^{\mathrm{m}} h_3 + h_3^{\mathrm{M}} q_3(0) - h_3^{\mathrm{M}} q_3^{\mathrm{m}})$; and $P_3^{(4)} = a_3(q_3^{\mathrm{M}} h_3 + h_3^{\mathrm{m}} q_3(0) - h_3^{\mathrm{m}} q_3^{\mathrm{M}})$ with $h_3^{\mathrm{m}} \leq h_3 \leq h_3^{\mathrm{M}}$. We notice in Fig. 4 that the constructed envelope provides a good approximation of the actual non-convex power output relationship given in (1). The solution obtained from (25), which is a linear approximation of the original problem (18) may be used to fix the main variables, especially those involved in nonlinear terms, and then solve the nonlinear original model or as an initial point of the original problem. In this case, we demonstrate that solving (25) is sufficient since one of the main nonlinear terms that introduces the biggest error is associated with the power output of the hydroelectric power system which provides a tight relaxation. In this regard, we calculate the difference between the power output of each hydroelectric system $P_{H_i}(t)$ as the output of the optimisation problem and the actual output of each hydroelectric system calculated using (1), i.e., $P_{\text{actual}_i}(t) = a_i h_i(t) q_i(t)$ for a period of a whole year; the results are shown in Table II. We define as the error ϵ_i the absolute difference of the actual and the approximated power output: $|P_{\text{actual}_i}(t) - P_{H_i}(t)|$; $\mathbb{E}[\epsilon_i]$ the mean value of the error; and σ_i the standard deviation. Furthermore, the maximum error for the total power output is 3.82 MW or 0.01 %. This accuracy could be further improved if instead of taking the head limits as defined in Table I; we follow this procedure: Given the starting volume of a reservoir determine the minimum and maximum head limits based on the maximum discharge rates. In this specific example following the aforementioned

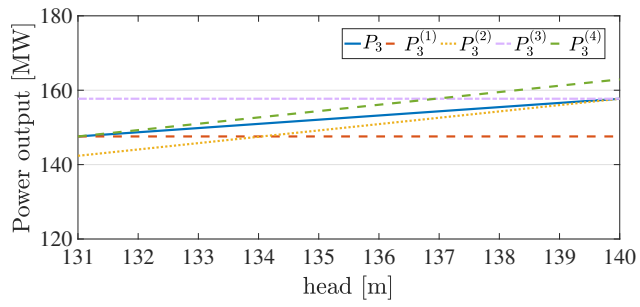

Fig. 4: Convex relaxation of Gitaru power for a given $q_3 = q_3(0)$.

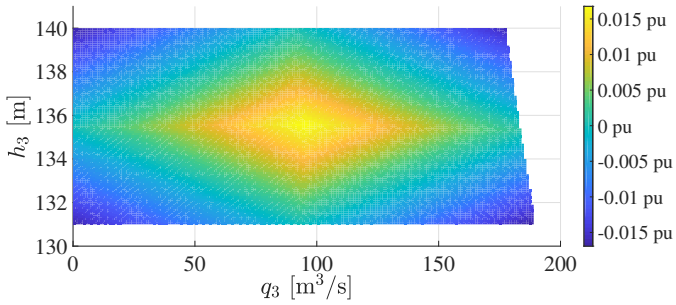

Fig. 5: Comparison of convex relaxation using McCormick's envelopes and a linear function fit to the three-dimensional hydropower production function.

procedure further decreases the error, e.g, the maximum error is now 1.41 MW instead of 3.82 MW. We compare the convex relaxation using McCormick's envelopes and a linear function fit to the three-dimensional hydropower production function denoted by $P_{\text{linear}} = \beta_0 + \beta_1 h + \beta_2 q$. By using the code developed by one of the paper's reviewers the coefficients for the Gitaru dam are $\beta_0 = -112.0754$ MW, $\beta_1 = 0.8277$ MW/m and $\beta_2 = 1.2216$ MW s/m^3. We then calculate the errors associated with each approximation, i.e., $\delta_1 = \frac{|P_{\text{actual}} - P_{\text{linear}}|}{P_3^{\text{M}}}$ and $\delta_2 = \frac{\min\{|P_{\text{actual}} - \min\{P_3^{(3)}, P_3^{(4)}\}|, |P_{\text{actual}} - \max\{P_3^{(1)}, P_3^{(2)}\}|\}}{P_3^{\text{M}}}$. In Fig. 5 we depict the difference $\delta = \delta_2 - \delta_1$, i.e., positive value means the linear fit is better than using McCormick's envelopes and vice versa. As it may be seen in the graph, the linear fit behaves better near the "centre" of the convex envelope and vice versa; the colour scale is in per unit.

The second step in the construction of the relaxed problem is to approximate the relationship between the head levels and the live volume, as described in Section IV-C. We use the data provided in [32] and in Fig. 6, we depict the actual relationship and the piecewise affine approximation between the head level and live volume for the Gitaru reservoir. As it may be seen the error introduced is marginal. For all the dams, we choose $K = 3$, i.e., we calculate the piecewise affine functions into three segments. For the five reservoirs we have:

$$
\begin{aligned}
h_1(t) &= 0.0281 v_1^1(t) + 0.0131 v_1^2(t) + 0.0084 v_1^3(t) + 25,\\
h_2(t) &= 0.3077 v_2^1(t) + 0.1351 v_2^2(t) + 0.0964 v_2^3(t) + 61,\\
h_3(t) &= 0.6349 v_3^1(t) + 0.4301 v_3^2(t) + 0.1667 v_3^3(t) + 131,\\
h_4(t) &= 0.5779 v_4^1(t) + 0.4117 v_4^2(t) + 0.2955 v_4^3(t) + 31,\\
h_5(t) &= 0.0648 v_5^1(t) + 0.0468 v_5^2(t) + 0.0398 v_5^3(t) + 134,
\end{aligned}
$$

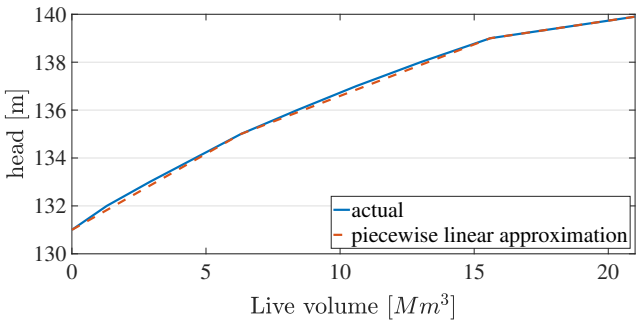

Fig. 6: Head level and live volume for Gitaru reservoir.

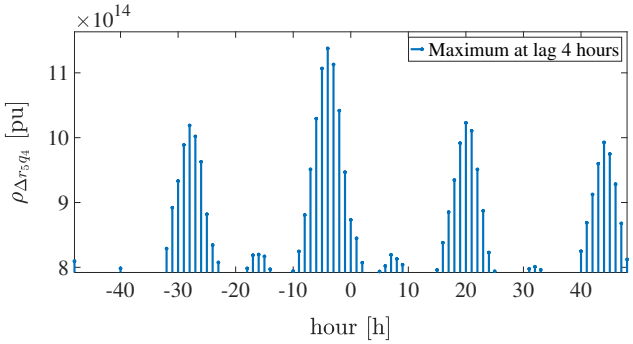

Fig. 7: Cross correlation coefficients between the net inflow of Kiambere and the water discharge of Kindaruma.

with $v_1^1(t) \in [0, 400], v_1^2(t) \in [0, 731], v_1^3(t) \in [0, 622]$; $v_2^1(t) \in [0, 14], v_2^2(t) \in [0, 37], v_2^3(t) \in [0, 82]$; $v_3^1(t) \in [0, 6], v_3^2(t) \in [0, 9], v_3^3(t) \in [0, 6]$; $v_4^1(t) \in [0, 4], v_4^2(t) \in [0, 3], v_4^3(t) \in [0, 3]$; and $v_5^1(t) \in [0, 292], v_5^2(t) \in [0, 137], v_5^3(t) \in [0, 90]$. The units for the live volumes are in Mm^3 and for the head in m.

B. Relaxed Optimal Dispatch

Kenya Electricity Generating Company (KenGen) provided hourly historical data of the power output of all the hydroelectric power output; dams head levels; and inflow data for all the hydroelectric power system from July 2015-June 2016. We used the power output model described in (1) to calculate the hourly water discharge rates $q_i(t)$ for $i = 1, \ldots, 5$ given the power output and the dam head levels. In (6)-(8), we wish to determine the time delay between all dams, i.e., τ_i, $i = 1, \ldots, 4$. We define a new parameter Δr_i, which is the net inflow of each dam and is defined as $\Delta r_i(t) = V_i(t) - V_i(t-1) + q_i(t)$, $i = 1, \ldots, 5$. We used the net inflow data of the dam i, i.e., $\Delta r_i(t)$, along with the water discharge data of the upstream dam $i-1$, i.e., $q_{i-1}(t)$ to calculate the time delay between dams. The rationale behind this idea is that the water discharge of the upstream dam usually is a big proportion of the inflow into the downstream dam; thus, we may determine how much time water needs to travel from one dam to the other. To this end, we calculate the cross-correlation of $\Delta r_i(t)$ and $q_{i-1}(t)$ for $i = 2, \ldots, 5$; the maximum of the cross-correlation function indicates the point in time where the signals are best aligned, i.e., the time delay between the two signals [34]. Thus, the time delay is equal to

$$
\tau_{i-1} = \underset{t'}{\text{argmax}} \Big\{ \rho_{\Delta r_i q_{i-1}}(t') = \sum_{t=1}^{T'} \Delta r_i(t) q_{i-1}(t + t') \Big\}, \tag{26}
$$

with $T' = 8760$ hours, since we have data for a one year period. The cross correlation coefficients between the net inflow of Kiambere ($i = 5$) and the water discharge of Kindaruma ($i = 4$) are depicted in Fig. 7. We may notice that the highest coefficient corresponds to time lag of 4 hours; thus based on (26) $\tau_4 = 4$ hours. We notice that there is also a 24 hour periodicity in the value of $\rho_{\Delta r_i q_{i-1}}(t')$. Based on similar analysis we have determined that the time delays are: Masigna-Kamburu, $\tau_1 = 2$ hours; Kamburu-Gitaru, $\tau_2 = 0 < 1$ hour; Gitaru-Kindaruma, $\tau_3 = 0 < 1$ hour; and Kindaruma-Kiambere, $\tau_4 = 4$ hours.

TABLE III: Tana river cascade system data.

Method	(B-i)	(B-ii)
Daily live volume [Mm^3]	2,006	2,070
Masinga participation [%]	6.7	6.9
Kamburu participation [%]	15.6	16.1
Gitaru participation [%]	37.8	31.7
Kindaruma participation [%]	12.2	8.5
Kiambere participation [%]	27.7	36.8

In the Tana river cascade there are three main inflow streams; in Masinga, Kamburu and Kiambere. The remaining inflow into the dams is due to rainfall data. The starting volume constraint for each reservoir is: $V_1(\text{start}) = 1173$ Mm^3; $V_2(\text{start}) = 118$ Mm^3; $V_3(\text{start}) = 13$ Mm^3; $V_4(\text{start}) = 4$ Mm^3; and $V_5(\text{start}) = 420$ Mm^3. There is no ending volume constraint.

In order to solve (25), we define $\overline{M}$ to be 10^8. We solve 365 times (25) (one for each day of the year) to determine the power output, live volume, head levels, spillage effects, and water discharge of all the dams in an hourly resolution. In order to test the performance of the proposed dispatch we compare the results between two methods: (B-i) dispatch proportional to the maximum capacity of each hydroelectric power plant; and (B-ii) proposed optimal hydroelectric power plant dispatch. A comparison of the results is shown in Table III. We notice from the results shown in Table III that the average daily live volume is a lot higher for method (B-ii) compared to (B-i). In this case study the national load curve, depicted in Fig. 2 was used, scaled to 500 MW; this results in an average daily load of $10,068$ MWh. The volume of water stored in the each dam in Mm^3 may be translated into live volume of water in MWh based on data provided to us by KenGen, which we refer to as average potential energy. This value is calculated based on the load in MWh that could be served by a dam if it was emptied with no additional inflow and is different than the maximum amount of energy that may be met by a dam as calculated using its maximum capacity. The increase in the average daily potential energy when operating the cascade with method (B-ii) was 5% higher than that of method (B-i) in order to meet the average daily load of $10,068$ MWh. Method (B-ii) tries to maximise the head levels; thus keeps the Gitaru head to high value increasing the dam's efficiency. It should be noted that Gitaru is the largest in capacity dam.

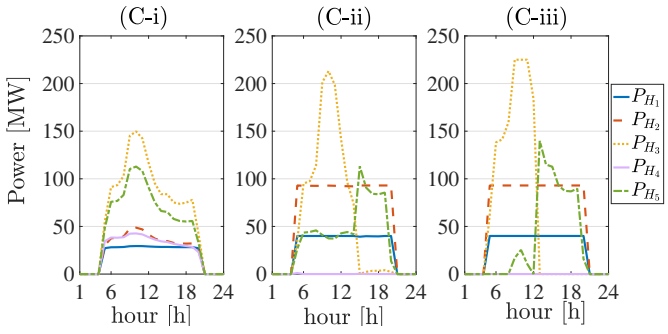

Fig. 8: Comparison of the power output of each hydroelectric power system for the three cases.

C. Comparison with other objective functions

We use the same set-up of the Tana river cascade to compare the results of different objective functions. However, the time horizon considered is one day and a constant inflow rate to the Masinga dam, i.e., $r_1 = 42$ m^3/s and $r_2 = r_3 = r_4 = r_5 = 0$ are taken into account. Based on the analysis given in [35] or [36], if costs are considered as an objective function these comprise of production costs and start-up costs. In the case of hydroelectric power systems, the production costs are negligible; thus the objective may be formulated as follows

$$\max \sum_{t=1}^{24} \sum_{i=1}^{5} (\lambda(t) P_{H_i}(t) - SU_i y_i(t)) + \sum_{i=1}^{5} Q_i V_i(t), \quad (27)$$

where $\lambda(t)$ is the forecasted price of energy in period t in \$/MWh; SU_i is the start-up cost of unit i in \$; $y_i(t)$ is a binary variable which is equal to 1 if hydroelectric power station i is started-up at the beginning of period t; and Q_i is the future value of the stored water in the reservoir associated with hydroelectric power plant i in \$/Mm^3. In this subsection, we consider three cases: (C-i) where we assume same start up costs for all units; set $Q_i = 0$; $\lambda(t) = 35$ \$/MWh for $t = 1, \ldots, 24$; (C-ii) where we assume same start up costs for all units; set $Q_i = 0.004$ \$/Mm^3; $\lambda(t) = 35$ \$/MWh for $t = 1, \ldots, 24$; and (C-iii) where we have the proposed maximisation of the head levels by avoiding spillage. In Fig. 8, we notice that as we place a value to the volume of the cascade, i.e., 0.004 \$/Mm^3 the solution of (C-ii) moves towards the solution of (C-iii); however if a smaller value was chosen then the solution of (C-ii) would be closer to that of (C-i).

D. Cascaded Hydro-Solar Hybrid Benefits

In order to quantify the benefits of a cascaded hydro-solar hybrid we use the proposed optimal dispatch scheme for various solar penetration levels, i.e., $0, 3, 10, 30$, and 100 MW. We use solar data from Solargis [37]. The coupling of hydroelectric power and solar systems is appropriate due to the negative correlation of solar and rainfall data. In Fig. 9, it may be seen that the inflow to Masinga dam was much lower in periods where the solar generation was high. The benefits of a cascade of a hydro-solar hybrid refer to both the amount of solar generation a system may accommodate as well as the increased live water volume in the dams. As it may be seen in Fig. 10 the higher the solar penetration levels the higher the potential available energy. The time elapsed to solve the optimisation problems for solar penetration levels of 0, 3, 10,

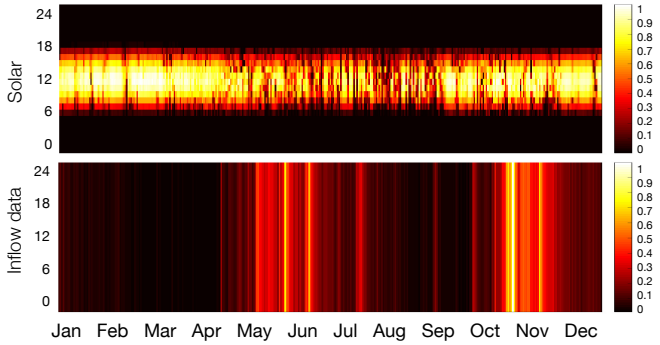

Fig. 9: Negative correlation of inflow data and PV output.

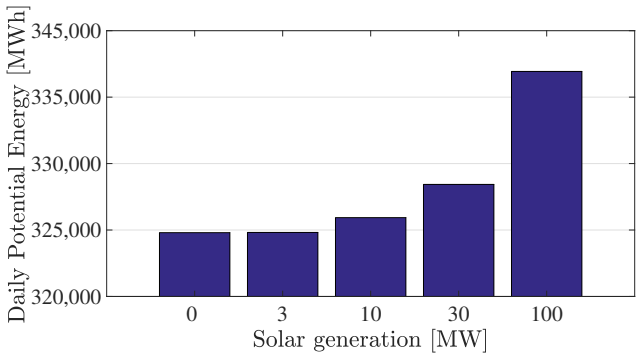

Fig. 10: Potential energy for various solar penetration levels.

30, and 100 MW was 66.90, 69.26, 64.65, 67.88, and 70.01 seconds respectively using a laptop with processor 3.3GHz Intel Core i7 and 16 GB RAM with the function *linprog* of MATLAB [38].

An interesting aspect of the cascaded hydro-solar hybrid systems is that they may be used to meet the growing demand in Kenya (e.g., [39]). We constraint the maximum capacity of solar generation to be 120% of the size of each hydroelectric power station. This is a heuristic measure to ensure that no problems will be created to the transmission system or transformer loadings due to the solar generation deployment. In this regard, we install solar generation of total 714 MW. We then determine the maximum amount of load that may be met with the cascaded hydro-solar hybrid. The maximum load that may be met is equal to 595 MW which is the maximum capacity of the hydroelectric power system. The reason behind this is that the peak demand occurs in the afternoon when there is not enough solar generation. However, the hydroelectric has to meet a smaller amount of load since part of it is met by the solar generation; thus increasing the live volume of the dams. In particular, the average daily potential energy is now 6% higher than the case with zero solar penetration. The baseline used to calculate the 6% increase in average daily potential energy was when the cascade was only used to meet the national load, scaled by 595 MW, for a one year period. This was compared to the case where the cascade plus solar generation of 714 MW is used to meet the same load. The operational dispatch scheme in both cases was the proposed methodology. This scenario was used to motivate the fact that in order to appropriately leverage the benefits of hydroelectric power and solar generation in years where there are enough inflows thus the "storage" of the cascade in terms of volume of water is not sufficient, additional storage devices or an increase in the load are necessary. In this case, since the net load is negative in several instances, the power balance constraint of (25) is modified to be $\sum_{i\in\mathcal{N}} P_{H_i}(t) = \max\{\Delta P_L(t), 0\}, \forall t \in \mathcal{T}$. The coupling of solar and hydro for one day in the year is depicted in Fig. 11. In order to leverage all the benefits of the cascaded hydro-solar hybrid there is a need for "storage" to store the spilled solar generation, as seen in Fig. 11. This may be achieved through pumped hydro or storage devices.

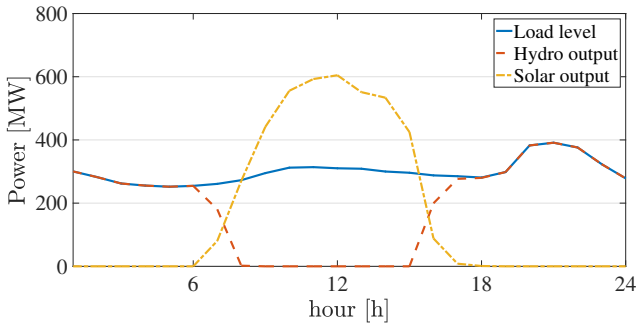

Fig. 11: Cascaded hydro-solar hybrid scheduling.

VI. Concluding Remarks and Extensions

In this paper, we addressed the question of maximising the energy per cubic meter of water in the cascaded hydro-solar hybrid system, by an optimal dispatch scheme. This requirement is becoming more important due to changes in climatic conditions. We constructed a nonlinear optimisation problem that represents explicitly the physical constraints of hydroelectric power systems. However, this optimisation problem took a significant time period to solve and did not guarantee a global optimum. Therefore, we relaxed the full nonlinear problem to a linear optimisation problem that is solvable for use in short-term operation of cascaded hydro-solar hybrid systems. We used McCormick's envelopes to construct convex envelopes around a bilinear function. Then, we used affine piecewise approximations to express the nonlinear relationship between head and live volume of each hydroelectric power system reservoir. Last, we exploited optimality properties to linearise the spillage effects constraints.

In the case study, we demonstrated that the proposed approximations provide an accurate description of the problem; and quantified the benefits of using the proposed dispatch compared to others in terms of available potential energy; live volume; and system efficiency. In particular, the increase in the average daily potential energy when operating the cascade with the proposed optimal dispatch was 5% higher than compared to a proportional to the maximum capacity dispatch in order to meet an average daily load of $10,068$ MWh. Moreover, we showed the advantages of a cascaded hydro-solar hybrid and identified some possible challenges. More specifically, the excess of water increases system flexibility in dry seasons; since the coupling of hydroelectric and solar technology is beneficial due to the negative correlation of rain and sunshine. An installation of 100 MW of solar resulted in 4% higher average daily potential energy. A 714 MW solar installation led to only 6% higher average daily potential energy, which means that there is a need for "storage" to store the spilled solar generation.

There are natural extensions of the work presented here. For instance, incorporating uncertainty sources into the forecasts of the net load that the hydroelectric power system is required to meet, i.e., uncertainty in the solar power and load variations may be investigated. Furthermore, the inclusion of cascaded hydro-solar hybrid systems in a larger power system to optimise the overall system performance should be pursued.

Acknowledgement

The authors would like to thank Kenya Electricity Generating Company for providing useful data for the case study and support in making this work possible. We wish to thank an anonymous reviewer for suggesting the analysis and providing the code to generate Fig. 5.

REFERENCES

[1] J. Delbeke and P. Vis, "EU Climate Policy Explained," European Union, Tech. Rep. 2011/833/EU.

[2] (2016, Aug.) New low solar price record set in chile – 2.91 per kwh! [Online]. Available: https://cleantechnica.com

[3] E. Ela, M. Milligan, and B. Kirby, "Operating reserves and variable generation," National Renewable Energy Laboratory, Tech. Rep. NREL/TP-5500-51978.

[4] Y. V. Makarov, C. Loutan, J. Ma, and P. de Mello, "Operational impacts of wind generation on california power systems," *IEEE Transactions on Power Systems*, vol. 24, no. 2, pp. 1039–1050, May 2009.

[5] M. Densing, S. Hirschberg, and H. Turton, *Review of Swiss Electricity Scenarios 2050: Report Prepared for the Group Energy Perspectives and the Swiss Competence Center for Energy Research "Supply of Electricity" (SCCER SoE)*, ser. PSI-Bericht. Paul Scherrer Institut PSI, 2014, no. ISSN 1019-0643.

[6] P. Karampelas and L. Ekonomou, *Electricity Distribution: Intelligent Solutions for Electricity Transmission and Distribution Networks*, ser. Energy Systems. Springer Berlin Heidelberg, 2016.

[7] I. Kougias, S. Szabó, F. Monforti-Ferrario, T. Huld, and K. Bódis, "A methodology for optimization of the complementarity between small-hydropower plants and solar PV systems," *Renewable Energy*, vol. 87, Part 2, pp. 1023 – 1030, 2016.

[8] R. Akikur, R. Saidur, H. Ping, and K. Ullah, "Comparative study of stand-alone and hybrid solar energy systems suitable for off-grid rural electrification: A review," *Renewable and Sustainable Energy Reviews*, vol. 27, no. C, pp. 738–752, 2013.

[9] A. Beluco, P. K. de Souza, and A. Krenzinger, "A dimensionless index evaluating the time complementarity between solar and hydraulic energies," *Renewable Energy*, vol. 33, no. 10, pp. 2157 – 2165, 2008.

[10] ——, "A method to evaluate the effect of complementarity in time between hydro and solar energy on the performance of hybrid hydro pv generating plants," *Renewable Energy*, vol. 45, no. Supplement C, pp. 24 – 30, 2012.

[11] J. Matevosyan, M. Olsson, and L. Söder, "Hydropower planning coordinated with wind power in areas with congestion problems for trading on the spot and the regulating market," *Electric Power Systems Research*, vol. 79, no. 1, pp. 39 – 48, 2009.

[12] A. Hamann and G. Hug, "Using cascaded hydropower like a battery to firm variable wind generation," in *IEEE Power and Energy Society General Meeting*, Jul. 2016, pp. 1–5.

[13] M. Santarelli and S. Macagno, "Hydrogen as an energy carrier in stand-alone applications based on PV and PV–micro-hydro systems," *Energy*, vol. 29, no. 8, pp. 1159 – 1182, 2004.

[14] A. V. Ntomaris and A. G. Bakirtzis, "Stochastic scheduling of hybrid power stations in insular power systems with high wind penetration," *IEEE Transactions on Power Systems*, vol. 31, no. 5, pp. 3424–3436, Sep. 2016.

[15] A. J. Wood and B. F. Wollenberg, *Power Generation, Operation, and Control*, ser. A Wiley-Interscience publication. Wiley, 1996.

[16] R. M. Lima, M. G. Marcovecchio, A. Q. Novais, and I. E. Grossmann, "On the computational studies of deterministic global optimization of head dependent short-term hydro scheduling," *IEEE Transactions on Power Systems*, vol. 28, no. 4, pp. 4336–4347, Nov. 2013.

[17] A. L. Diniz and M. E. P. Maceira, "A four-dimensional model of hydro generation for the short-term hydrothermal dispatch problem considering head and spillage effects," *IEEE Transactions on Power Systems*, vol. 23, no. 3, pp. 1298–1308, Aug. 2008.

[18] Y. Zhu, J. Jian, J. Wu, and L. Yang, "Global optimization of non-convex hydro-thermal coordination based on semidefinite programming," *IEEE Transactions on Power Systems*, vol. 28, no. 4, pp. 3720–3728, Nov. 2013.

[19] M. Cordova, E. Finardi, F. Ribas, V. de Matos, and M. Scuzziato, "Performance evaluation and energy production optimization in the real-time operation of hydropower plants," *Electric Power Systems Research*, vol. 116, pp. 201 – 207, 2014.

[20] J. W. Labadie, "Optimal operation of multireservoir systems: State-of-the-art review," *Journal of Water Resources Planning and Management*, vol. 130, no. 2, pp. 93–111, 2004.

[21] B. Gatner and J. Matousek, *Approximation Algorithms and Semidefinite Programming*. Springer-Verlag Berlin Heidelberg, 2012.

[22] J. P. S. Catalao, S. J. P. S. Mariano, V. M. F. Mendes, and L. A. F. M. Ferreira, "Scheduling of head-sensitive cascaded hydro systems: A nonlinear approach," *IEEE Transactions on Power Systems*, vol. 24, no. 1, pp. 337–346, Feb. 2009.

[23] R. Moraga, J. Garcia-Gonzalez, S. Nogales, and M. Arteseros, "A contingency analysis for managing the risk of water spillage and shortage in a mid-term hydro scheduling model," in *2006 International Conference on Probabilistic Methods Applied to Power Systems*, Jun. 2006, pp. 1–6.

[24] P. C. Sharma and A. R. Abhyankar, "Multi-objective short-term tandem hydro scheduling: MINLP approach," in *2016 IEEE 1st International Conference on Power Electronics, Intelligent Control and Energy Systems (ICPEICES)*, Jul. 2016, pp. 1–6.

[25] D. Apostolopoulou, Z. D. Greve, and M. McCulloch, "Robust optimization for hydroelectric system operation under uncertainty," *IEEE Transactions on Power Systems*, vol. 33, no. 3, pp. 3337–3348, May 2018.

[26] T. Stokelj, D. Paravan, and R. Golob, "Short and mid term hydro power plant reservoir inflow forecasting," in *International Conference on Power System Technology*, vol. 2, 2000, pp. 1107–1112.

[27] M. Mbuthia, "Hydroelectric system modelling for cascaded reservoir-type power stations in the lower tana river (seven forks scheme) in kenya," in *3rd AFRICON Conference*, Sep. 1992, pp. 413–416.

[28] S. Grin, "Geometry and area depth volume curves of the reservoirs in the semiarid madalena basin in northeast brazil," University of Twente, Tech. Rep. S1232533.

[29] A. L. Diniz, "Test cases for unit commitment and hydrothermal scheduling problems," in *IEEE PES General Meeting*, Jul. 2010, pp. 1–8.

[30] F. A. Al-Khayyal and J. E. Falk, "Jointly constrained biconvex programming," *Mathematics of Operations Research*, vol. 8, no. 2, pp. 273–286, 1983.

[31] I. Griva, S. G. Nash, and A. Sofer, *Linear and Nonlinear Optimization: Second Edition*. Society for Industrial and Applied Mathematics (SIAM, 3600 Market Street, Floor 6, Philadelphia, PA 19104), 2009.

[32] T. of Lahmeyer International, "Development of a power generation and transmission master plan, kenya," Ministry of Energy and Petroleum, Republic of Kenya, Tech. Rep. v20161128, May 2016.

[33] J. B. Orlin, "Optimization methods in business analytics, integer programming," Massachusetts Institute of Technology, Tech. Rep. Chapter 9.

[34] U. Yule, "Why do we sometimes get nonsense-correlations between time series? –a study in sampling and the nature of time series," in *Journal of the Royal Statistical Society*, 1926, pp. 1–63.

[35] A. J. Conejo, J. M. Arroyo, J. Contreras, and F. A. Villamor, "Self-scheduling of a hydro producer in a pool-based electricity market," *IEEE Transactions on Power Systems*, vol. 17, no. 4, pp. 1265–1272, Nov. 2002.

[36] O. Nilsson and D. Sjelvgren, "Variable splitting applied to modelling of start-up costs in short term hydro generation scheduling," *IEEE Transactions on Power Systems*, vol. 12, no. 2, pp. 770–775, May 1997.

[37] (2017, Mar.) Solar resource overview, kenya. [Online]. Available: http://solargis.com/products/pvplanner/overview/

[38] (2017, Nov.) Solve linear programming problems. [Online]. Available: https://uk.mathworks.com/help/optim/ug/linprog.html

[39] "Updated least cost power development plan, study period: 2011-2031," REPUBLIC OF KENYA, Tech. Rep., Mar. 2011.

Dimitra Apostolopoulou was awarded a Ph.D. and a M.S. in Electrical and Computer Engineering from University of Illinois at Urbana-Champaign in 2014 and 2011, respectively. She received her undergraduate degree in Electrical and Computer Engineering from National Technical University of Athens, Greece in 2009. She is currently a Lecturer at City, University of London. Previously, she was a Postdoctoral researcher at University of Oxford and a Lecturer at Christ Church College. Priorly, she worked at the Smart Grid and Technology Department at Commonwealth Edison Company. Her research interests include power system operations and control, market design and economics.

Malcolm McCulloch was born in South Africa. He received the B.Sc. (Eng.) and Ph.D. degrees in electrical engineering from the University of Witwatersrand, Johannesburg, South Africa, in 1986 and 1990, respectively. In 1994, he headed up the Energy and Power Group, University of Oxford, Oxford, U.K., where he has been active in the areas of electrical machines, transport, and smart grids. He is the Co-Director of the Oxford Martin Programme on Integrating Renewables. Malcolm has active research programmes in the four sectors of developing world, domestic, transport and renewable generation. Malcolm has spun out four for profit companies and two not for profit enterprise. He has over 120 publications and over 20 patent and patent applications.